Angewandte Chemie
GDCh
Eine Zeitschrift der Gesellschaft Deutscher Chemiker
www.angewandte.de

Akzeptierter Artikel

Titel: Hydrogen-Bond Free Energy of Local Biological Water

Autoren: Won-Woo Park, Kyung Min Lee, Byeong Sung Lee, Young Jae Kim, Se Hun Joo, Sang Kyu Kwak, Tae Hyeon Yoo, and Oh-Hoon Kwon

Zitierweise: *Angew. Chem. Int. Ed.* 10.1002/anie.202002025
Angew. Chem. 10.1002/ange.202002025

Link zur VoR: http://dx.doi.org/10.1002/anie.202002025
http://dx.doi.org/10.1002/ange.202002025

WILEY-VCH

10.1002/ange.202002025

WILEY-VCH

RESEARCH ARTICLE

Hydrogen-Bond Free Energy of Local Biological Water

Won-Woo Park[a], Kyung Min Lee[b], Byeong Sung Lee[c], Young Jae Kim[a,d], Se Hun Joo[b], Sang Kyu Kwak*,[b], Tae Hyeon Yoo*,[c], and Oh-Hoon Kwon*,[a,d]

Abstract: Here, we propose an experimental methodology based on femtosecond-resolved fluorescence spectroscopy to measure the hydrogen (H)-bond free energy of water at protein surfaces under isothermal conditions. A demonstration was conducted by installing a non-canonical isostere of tryptophan (7-azatryptophan) at the surface of a coiled-coil protein to exploit the photoinduced proton transfer of its chromophoric moiety, 7-azaindole. The H-bond free energy of such biological water was evaluated by comparing the rates of the proton transfer, sensitive to the hydration environment, at the protein surface and in bulk water, and it was found to be higher than that of bulk water by 0.4 kcal/mol. The free-energy difference is dominated by the entropic cost in the H-bond network among water molecules at the hydrophilic and charged protein surface. Our study opens a door to accessing the energetics and dynamics of local biological water to give insight its roles in protein structure and function.

Introduction

Water present in the vicinity of biological macromolecules, called "biological water," plays a critical role in the structural stability and dynamics of associated macromolecules and can thereby modulate their functions.[1] These water molecules also participate in the interactions between biological entities and various other molecules ranging in size from small to very large and determine the binding affinity to proteins.[2]

The behavior of biological water is unique compared to that of water in bulk. This is because the hydrogen (H)-bonds among biological water molecules are either partly replaced by bonds to a hydrophilic protein surface or limited due to the topology and hydrophobicity of the protein surface,[3] either of which produces a diverse array of physicochemical properties. It is therefore desirable to characterize biological water at the molecular level in terms of its mobility, which is primarily controlled by H-bond breakage and H-bonding energy, and other factors.

Many researchers have investigated hydration *dynamics* in biological systems from experimental and theoretical perspectives to address the nature of the interactions and associated dynamics between water and protein molecules.[4] In contrast, the *energetics* of the H-bonds in biological water have largely been ignored even though these are fundamental to understanding the foundations of hydration at biological surfaces towards designing and controlling biological function. Recently, the Zhong group successfully obtained activation energies for hydration of proteins originating from several different environments by invoking the Arrhenius relationship, which requires rates to be measured at a series of temperatures.[4b] However, interpreting the activation energies obtained from such analyses is not straightforward in cases where not only the energy available to populate a reactive configuration along a reaction coordinate but other factors, such as the conformation of a protein, depend on temperature.

Here, we report a new experimental approach to elucidate the H-bond free energy of biological water at protein surfaces under isothermal conditions using a fluorescent hydration probe of prototropic chemical reactivity. Studying the energetics and dynamics of biological water will expand our understanding the role of water in biological assembly and biochemical processes, *e.g.*, maintaining and modulating ligand binding.[2] This work promises the mapping of such the properties of local biological water to predict and design functional biological entities.

Model system

The non-canonical amino acid 7-azatryptophan (AW) (Figure 1a) was selected as it has a similar molecular structure and size as tryptophan (W) but exhibits unique H-bond interactions with adjacent water molecules. Another advantage is that the photochemistry of the chromophoric moiety of AW, or 7-azaindole (7AI), has been extensively investigated.[5, 6]

The excited-state prototropy of 7AI involves a parent normal form (N*) and a proton-translocated tautomer (T*). The excited-state proton transfer (ESPT) of 7AI has been reported to occur via catalysis by a water molecule, which produces a transient 1:1 cyclical H-bonded complex with N* (N*‡) from a more stable noncyclical H-bonded complex.[6] The efficiency of ESPT depends on the free-energy difference ($\Delta G^{\ddagger}$) between the well-configured N*‡ and the prevalent noncyclical H-bonded 7AI-water complexes, as depicted in Figure 1b. The overall rate of ESPT (k_{PT}) can be computed as:[6]

$$k_{PT} = k_{pt} \exp(-\Delta G^{\ddagger}/k_B T), \quad (1)$$

where k_{pt} is the intrinsic rate for proton dissociation, k_B is the Boltzmann constant, and T is the temperature in Kelvin.

[a] W.-W. Park, Y. J. Kim, Prof. Dr. O.-H. Kwon
Department of Chemistry, School of Natural Science
Ulsan National Institute of Science and Technology
Ulsan 44919 (Republic of Korea)
E-mail: ohkwon@unist.ac.kr
[b] K. M. Lee, S. H. Joo, Prof. Dr. S. K. Kwak
Department of Energy Engineering, School of Energy and Chemical Engineering
Ulsan National Institute of Science and Technology
Ulsan 44919 (Republic of Korea)
[c] Dr. B. S. Lee, Prof. Dr. T. H. Yoo
Department of Molecular Science and Technology
Ajou University
Suwon 16499 (Republic of Korea)
[d] Y. J. Kim, Prof. Dr. O.-H. Kwon
Center for Soft and Living Matter
Institute for Basic Science (IBS)
Ulsan 44919 (Republic of Korea)

Supporting information for this article is given via a link at the end of the document.

10.1002/ange.202002025

WILEY-VCH

RESEARCH ARTICLE

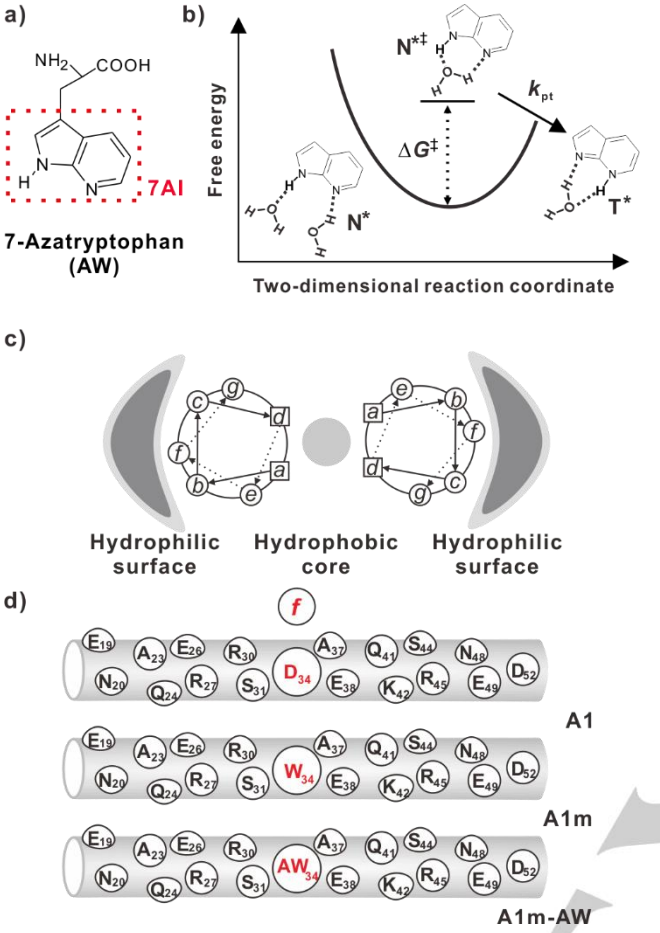

Figure 1. Schematics of the prototropy of the fluorescent probe and the structures of model proteins. (a) Molecular structure of AW. (b) Schematic energetics of the two-step excited-state proton transfer model of 7AI. (c) Top view of the coiled-coil model proteins in this study. (d) Side views of A1, A1m, and A1m-AW proteins. For A1, A1m, and A1m-AW, the residues at 34 positions were aspartic acid (D), tryptophan (W), and 7-azatryptophan (AW), respectively.

To achieve a cyclical H-bonded configuration in water, the complexing water molecule should replace one H-bond to an adjacent water molecule with a new H-bond to 7AI, as shown in Figure 1b. When the chromophoric moiety is installed at an appropriate position in a protein, for example one exposed to bulk water, the difference in the H-bond free energy between biological and bulk water can be determined by comparing the k_{PT} values on and off the protein surface. In this study, AW was selected and inserted in a model protein to probe the energetics and dynamics of water H-bonds based on the ESPT of the 7AI moiety. In the control experiment, AW was replaced with W because this amino acid has a similar molecular structure and can be used to probe hydration but does not undergo the ESPT.

The engineered coiled-coil protein A1 was selected as the model based on its structural integrity to guarantee the maximum exposure of the hydration probes to water after insertion (Figure 1c).[4c, 7] The secondary structure of A1 is α-helix with six copies of seven repeating amino acids that can be described as $(abcdefg)_n$, where each letter represents a different amino acid. In aqueous solutions, the hydrophobic residues at positions *a* and *d* of different A1 monomers cluster to form a hydrophobic core inside the coiled-coil protein. Note that the original A1 protein does not contain aromatic fluorescent residues that absorb ultraviolet (UV) light above 280 nm, such as tyrosine or W.[4c, 7] A residue at *f* position (D34) highly exposed to water was changed by W (A1m), which had previously been used to study the hydration dynamics (Figure 1d).[4c] Here, also prepared was A1m-AW, in which W was replaced by AW in a residue-specific manner.

Structural Characterization

The presence of the hydration probes of W and AW at position 34 (*f* position in the heptad) of the A1 protein was confirmed via the absorption spectra shown in Figure 2a. The lowest absorption maxima were at approximately 280 and 290 nm for A1m and A1m-AW, respectively, which are similar to those of bare W and AW in water.

The circular dichroism (CD) spectra of the two coiled-coil proteins are shown in Figure 2b, where it can be seen that both maintain α-helix structures. Using the K2D3 software package,[8] the helicities of A1m and A1m-AW were estimated to be 52% and 57%, respectively, which are comparable to the α-helicity of A1m described in a previous report.[4c] This suggests more than half of the amino acids in both A1m and A1m-AW are in regions containing α-helix secondary structures.

Based on these results, the structures were confirmed to be predominantly α-helical and to form a rigid coiled-coil structure, which maximizes the chances of exposing the hydration probes to water when their positions are properly chosen. Here, the hydration probes were installed at the most surface-exposed position on the coiled-coil protein, the *f* position (residue 34) in the middle of the A1 protein.

The extent of exposure of the W and AW residues to water can be estimated from the steady-state fluorescence spectra of A1m and A1m-AW.[9] It has been well established that the fluorescence maximum of the W residue ranges from approximately 320 nm, when deeply buried in proteins, to 350 nm in cases where the residue is fully exposed to an aqueous environment. As shown in Figure 2c, the fluorescence maxima of both W and A1m were located near 350 nm. This indicates that the installation of W at the surface-exposed aspartic acid of the *f* position of the third heptad (residue 34) in the middle of the rigid α-helix chain was a successful approach that ensured the maximum exposure of the chromophore to biological water. These results are consistent with previous results.[4c]

When evaluated, the emission maxima of AW and A1m-AW differed significantly, *i.e.*, 400 nm for AW and 387 nm for A1m-AW. This does not seem to agree with our original design of the A1m-AW protein. The spectral full width at half maximum (FWHM) of A1m-AW was significantly larger (~6000 cm^{-1}) than that of AW (~5000 cm^{-1}). By the spectral deconvolution of the time-resolved fluorescence spectra of A1m-AW based on a global-lifetime analysis (Figure 2c), two bands with different lifetimes can be seen, one of which decays in 2.2 ns with a peak at 360 nm and another that relaxes much faster (~0.4 ns) and has a peak at 400 nm. The spectral width of the 0.4-ns component was ~5100 cm^{-1}, which is similar to that of bare AW. As the integrated area of the

10.1002/ange.202002025

WILEY-VCH

RESEARCH ARTICLE

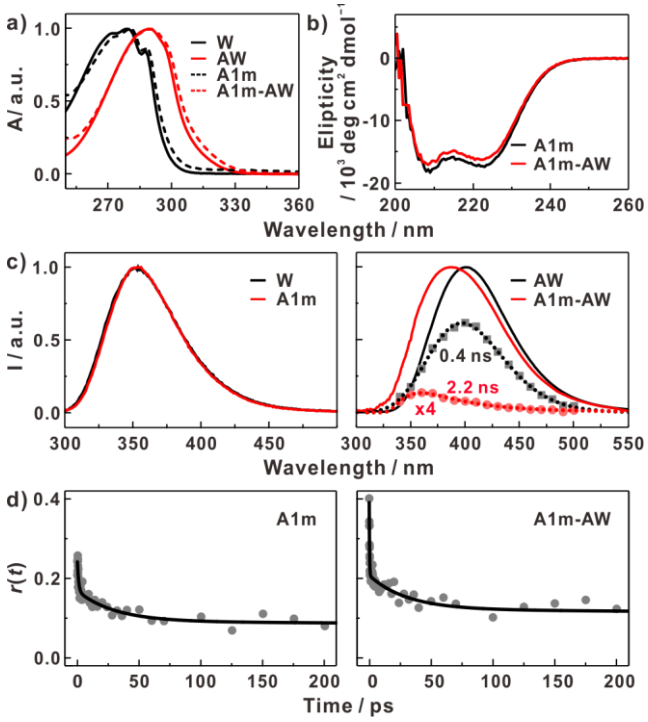

Figure 2. Structural characterization. (a) Steady-state UV-visible absorption spectra of W, AW, A1m, and A1m-AW. (b) CD spectra of both proteins. (c) Fluorescence spectra of W and A1m (left panel), and, AW and A1m-AW (right panel) obtained via excitation at 285 nm. In the right panel, spectral deconvolution of the time-resolved fluorescence spectra obtained by the time-correlated single photon counting (TCSPC) measurements reveals the two bands of different peak having the global lifetimes of 0.4 ns (black squares) and 2.2 ns (red circles). (d) Time-resolved anisotropy $r(t)$ of A1m (left panel) and A1m-AW (right panel). Depicted lines are the fit curves according to tri-exponential decay: $r(t) = \sum_i^3 r_i \exp(-t/\tau_i)$.

360-nm band was approximately 5% of that of the 400-nm band, it was inferred that the majority of the AW residue was fully exposed to water because it exhibited the same fluorescence maximum as that of bare AW in the same buffer solution. The origin of the 360-nm band was conjectured to be the minor conformation of the AW residue, which may experience a crowded environment due to adjacent residues and cause water to be expelled from the proximity. In a reverse micellar environment with a trace amount of water, AW was reported to exhibit a fluorescence peak at 370 nm.[10]

Based on the fact that the amplitudes of the two different lifetime components are positive across the wavelength range of their bands, the two conformations do not seem to interchange within their excited-state lifetimes. It follows that the ground-state equilibrium between the two conformations determines their fractions. Because the majority (95%) of the AW residue was fully exposed to biological water while the AW residue undergoes ESPT only when exposed to water, the ESPT rates of AW and the major conformer of A1m-AW in the same buffer solutions can be compared to determine the H-bond free energy of biological water.

The local environments around the probes can also be investigated in terms of their mobility. The depolarization dynamics related to the motion of the W and AW residues were obtained by measuring the femtosecond (fs)-resolved fluorescence anisotropy as shown in Figure 2d. Upon analysis, three distinct timescales were identified that ranged from hundreds of fs to a few picoseconds (ps), tens of ps, and several nanoseconds (ns), longer than our time window, as given in Table S1. The initial ultrafast components were attributed to internal conversion between two adjacent excited electronic states of the probes. The second decay components originated from local wobbling due to the restricted motion of the probe residue and the slowest components were ascribed to protein tumbling motions.[4b,c,f, 11] Using the previously reported wobble-in-a-cone model,[4b,c,f, 12] the cone semiangles, within which the W and AW residues wobbled, were determined to be 24° ± 2° and 23° ± 2°, respectively, which are consistent with the previously reported value (21°) for A1m.[4c] This result indicates that the W and AW residues were in similar local structural environments.

A molecular dynamics (MD) simulation was conducted to determine the structural integrities of the A1m and A1m-AW proteins. First, the structural characteristics of the hydrated A1m and A1m-AW proteins were probed by monitoring the root mean square displacement (RMSD) and root mean square fluctuation (RMSF) for 50 ns from the initial model structures. Both proteins underwent large structural changes from their initial structures but eventually converged to their equilibrium structures in ~25 ns (Figure 3a). The RMSF was analyzed over the last 25 ns of the trajectory to confirm the stability of the coiled-coil structure of the proteins (Figures 3b, c, and d). It was found that in both proteins, the residues in positions ranging from 15 to 56, which constituted α-helical coiled-coil structure, had lower RMSF values, as anticipated for a rigid coiled-coil structure. Second, the possibility for W and AW residues to be exposed to water was investigated. The average conformations of the W and AW residues during the last 25 ns of the trajectory indicated that both W and AW had stretched-out conformations toward the opposite side of the hydrophobic core (Figure S1). This maximized the probability of

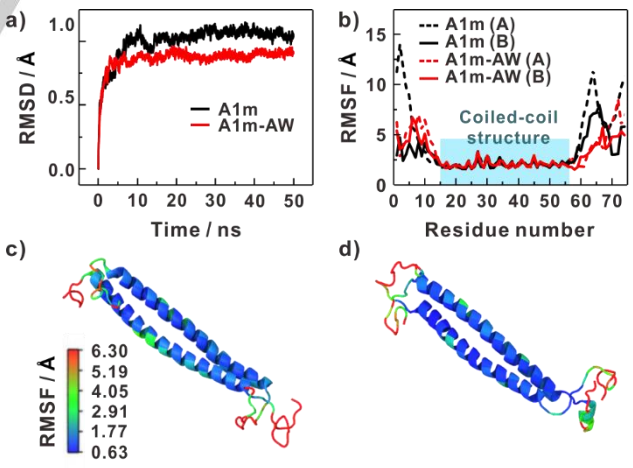

Figure 3. Simulated coiled-coil structures of hydrated A1m and A1m-AW. (a) Root mean square displacement (RMSD) of A1m and A1m-AW compared to their initial structures during the first 50 ns. The values converged to their equilibrium structures in ~25 ns. (b) Root mean square fluctuation (RMSF) of A1m and A1m-AW over the last 25 ns of the MD trajectories. Each coil in the same pair of the coil is denoted as (A) and (B). (c) and (d) RMSF values plotted on the average structure of A1m (c) and A1m-AW (d). The low RMSF value represents the high rigidity of the protein residues.

10.1002/ange.202002025

WILEY-VCH

the probe being exposed to water, as was intended. We also analyzed the possibility of the exposure by counting the average number of intermolecular H-bonds of the W and AW residues per timeframe (Table S2). The average number of intermolecular H-bonds per timeframe was similar to the number of possible H-bond sites in each residue. Next, to verify the W and AW residues were in similar local environments, the structural features of the hydrated residues were compared by computing the radial distribution function (RDF) of the oxygen atoms in the water in the vicinity of the exposed residues (Figure S2a). For both proteins, the RDF had the same distribution with a small peak at around 2 Å and a broad peak at 4 Å, indicating the presence of H-bonds and the first hydration layer, respectively. Therefore, we concluded that the probe residues had similar local hydration structures. Finally, the wobbling motion of the hydrated residues were compared by analyzing the distribution of dihedral angles χ_1 and χ_2 (Figures S2b, c, and d); it was found that in both proteins, the dihedral angles χ_1 and χ_2 were mainly distributed in the range of −150° to 150°, which indicates the wobbling motion of the exposed probe residues were limited in a similar manner.

The spectroscopic and mobility features as well as the results of the MD simulation presented in this section can be leveraged to stringently compare the ESPT dynamics between the pair of fluorophores AW and A1m-AW and the hydration dynamics between the two proteins A1m and A1m-AW.

Hydrogen-Bond Free Energy

The ESPT dynamics of AW and A1m-AW were analyzed via the irreversible two-state model presented in Scheme 1.[6] In this model, the formation of the prerequisite 1:1 cyclically H-bonded configuration (N*‡) is energetically unfavorable (transition state) such that the preequilibrium between the noncyclical H-bonded N* and N*‡ is exclusively biased toward the former. Here, k_{pt} is related to the intrinsic electronic property of the chromophoric moiety of AW (7AI). For bare AW and AW-containing polypeptides (trimer and octamer), the lowest singlet-transition energies in absorption and emission have been reported to be the same within the margin of 1 nm.[13] According to our quantum chemical calculation using density functional theory, AW and a trimer (E-AW-E) as a comparison showed almost identical nuclear geometries and partial charge distributions in the excited states (Figure S3). The vertical excitation energies were obtained to be nearly the same as well. All combined, it is inferred that the covalent peptide bonds to AW do not perturb the intrinsic electronic property of its chromophoric moiety, responsible for the ESPT. Therefore, k_{pt} can be considered to be the same for both

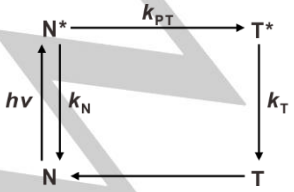

Scheme 1. Two-state excited-state proton transfer model of 7AI in water.

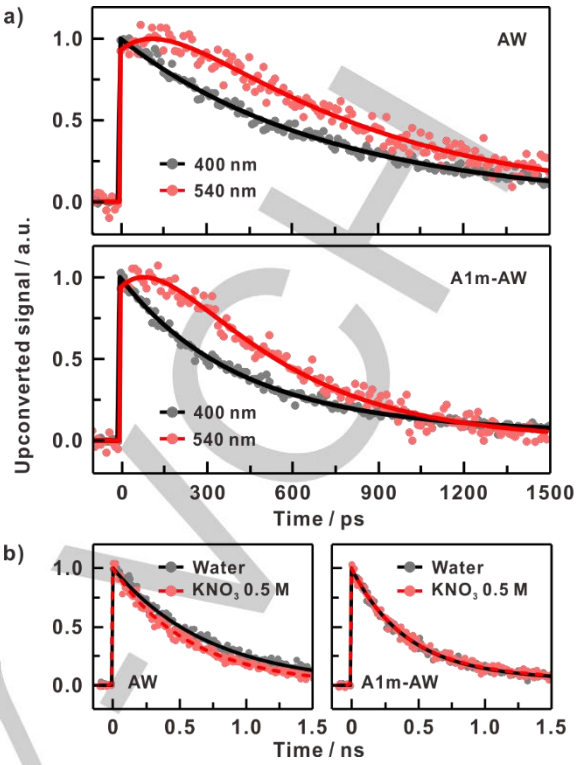

Figure 4. Fluorescence kinetic profiles of AW and A1m-AW representing excited-state proton transfer. The excitation wavelength was 285 nm. (a) Time-resolved fluorescence (symbol) of AW (upper panel) and A1m-AW (lower panel) measured at 400 nm (black) and 540 nm (red). The profiles were measured at 400 nm to trace the temporal dependence of [N*] and at 540 nm to trace [T*]. (b) Time-resolved fluorescence of AW (left panel) and A1m-AW (right panel) without (black) and with 0.5 M KNO_3 (red). All transients were fitted to $I(t) = \sum_i A_i \exp(-t/\tau_i)$ convoluted with the Gaussian instrument response function (IRF) of 250 fs (FWHM). The fit curves are also given in each panel as solid lines (and dashed lines as well in panel b).

A1m-AW and AW. Note that the typical value for k_{pt} is (100 fs)$^{-1}$. The temporal dependence of [N*] and [T*] can be determined as:

$$[N^*] = [N^*]_0 \exp[-(k_N + k_{PT})t], \quad (2)$$

$$[T^*] = [N^*]_0 \frac{k_{PT}}{k_N + k_{PT} - k_T}\{\exp(-k_T t) - \exp[-(k_N + k_{PT})t]\}, \quad (3)$$

where k_N and k_T are the rate constants for the relaxation of N* and T* apart from the ESPT, respectively. In this case, the overall ESPT rate, k_{PT}, depends on the free-energy difference ($\Delta G^{\ddagger}$) between N* and N*‡ as given in Figure 1b and Equation (1). Because k_T is greater than ($k_N + k_{PT}$) as evidenced by the absence of the steady-state fluorescence of T* above 500 nm (and as reported[6b, 14]), the apparent rise time of Equation (3) is represented by $(k_T)^{-1}$ while the apparent decay time by $(k_N + k_{PT})^{-1}$. The value of $(k_N)^{-1}$ was taken to be 18 ns, which is the lifetime (τ) of N* in polar aprotic dimethyl sulfoxide without ESPT (Figure S4). We note that according to the relationship of fluorescence lifetime with absorption intensity by Strickler and Berg[15] $(k_N)^{-1}$ is calculated to be ~16 ns in water (see Supporting Information).

To obtain the k_{PT} values for AW and A1m-AW, fs-resolved fluorescence transients were collected at 400 nm, which reflect the time-dependent populations of N* (Figure 4a). The transient

10.1002/ange.202002025

for AW was fitted to a single exponential decay with τ = 729 ± 5 ps. For A1m-AW, the main decay time was found to be 403 ± 11 ps with a minor long decay component with τ = 2.2 ns, which was ascribed to the lifetime of N* when crowded by adjacent residues with minimal exposure to water. These major time constants were found to be the same as the decay times of the T* fluorescence obtained at 540 nm; the rise time of 160 ps for both AW and A1m-AW corresponds to $(k_T)^{-1}$. The k_{PT} values for A1m-AW ($k_{PT,bio}$) and that for AW ($k_{PT,bulk}$) were deduced using the relationship of $1/\tau = k_{PT} + k_N$, where k_N is the total relaxation rate without k_{PT}. If $k_{PT,bio}$ is compared to $k_{PT,bulk}$, the difference between the H-bonding free energy ($\Delta\Delta G = \Delta G_{bio}^{\ddagger} - \Delta G_{bulk}^{\ddagger}$) of biological water and that of bulk water can be elucidated as:

$$k_{PT,bio}/k_{PT,bulk} = \exp(-\Delta\Delta G/k_B T). \quad (4)$$

Finally, the $\Delta\Delta G$ value was found to be −0.36 (±0.02) kcal/mol, which is significant compared to the H-bond free energy of water in bulk at 298 K (ΔG_{bulk} = 1–1.3 kcal/mol).[16]

The smaller free-energy difference between N* and N*‡ for A1m-AW indicates that at the protein surface, the formation of the activated complex, N*‡ is more facile compared to that in bulk. The major difference in the comparison set is the presence of hydrophilic residues around the probe. In the formation of N*‡, it is essential for a water molecule already singly H-bonded to a 7AI moiety to replace an H-bond to an adjacent water molecule with a new H-bond to the 7AI moiety. This is accompanied by breaking and forming H-bonds among nearby water molecules. It follows that the difference in the free-energy change ($\Delta\Delta G$) represents the difference of the H-bond free energy of biological water from that of water in bulk. The H-bond breakage and formation at the prototropic sites of the 7AI moiety are identical in both cases that they contribute little to $\Delta\Delta G$.

As a proof-of-principle experiment, we obtained the k_{PT} value for AW in the presence of a chaotrope (0.5 M),[17] nitrate (NO_3^-), in the buffer solution (Figure 4b). The ionic chaotrope was found to disrupt H bonds among water molecules accelerating the ESPT, decreasing τ from 729 ± 5 ps to 585 ± 6 ps, *i.e.*, destabilization of the H-bond free energy of water by 0.13 ± 0.01 kcal/mol. When the same amount of the chaotrope was dissolved in the A1m-AW solution, the k_{PT} value did not change. This implies that the H-bond network of biological water was already too ruptured to respond to the chaotrope or the effect of the chaotrope was local at the heterogeneous protein surfaces.

Hydration Dynamics

To visualize the motion of local biological water, we applied the time-resolved spectral reconstruction method demonstrated by the Zhong group (as detailed in the SI, Figures S5-S8).[18] The hydration energy relaxation, $\Delta\nu(t)$, was constructed as:

$$\Delta\nu(t) = \nu^h_{max}(t) - \nu^h_{max}(\infty), \quad (5)$$

where $\nu^h_{max}(\infty)$ represents the emission maximum in wavenumbers after hydration is complete. To adequately fit $\Delta\nu(t)$ as in Figure 5, tri-exponential functions were used for all samples. The details of the fitting parameters are presented in Table S3.

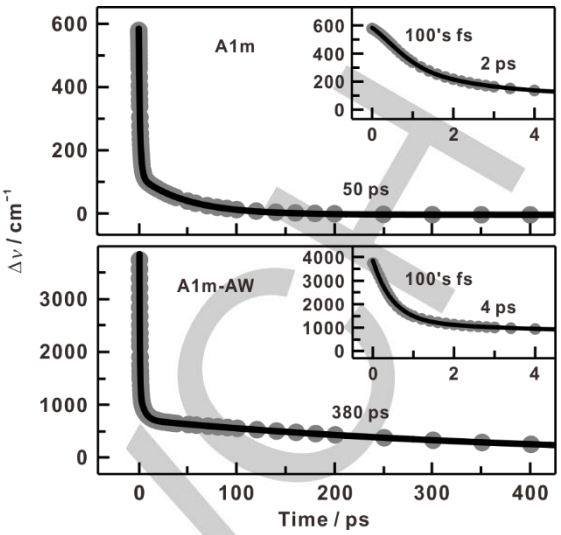

Figure 5. Hydration dynamics. Solvation correlation functions of A1m (upper panel) and A1m-AW (lower panel). Depicted lines are the fit curves. Details of reconstruction method and fitting parameters are given in Supporting Information.

The three distinct timescales were identified as 0.4–0.9, 1.7–3.7, and 50–380 ps for both proteins. As per several published studies,[4b,c,f, 19] the ultrafast component represents the motion of the water molecules in the outer hydration shells. The water molecules in the inner hydration shell reorient on a slower timescale of several ps. The slowest components with tens to several hundred of ps have been ascribed to water-protein collective rearrangements.

The results in Figure 5 and Table S3 can be summarized as follows. First, when the hydration dynamics of A1m-AW were compared to those of AW, the extent of the hydration energy relaxation was found to be larger than that of AW by ~2300 cm^{-1}, which indicates that a large fraction of the relaxation due to the hydration of AW in bulk water was missing because the relaxation was much faster than our time resolution of 250 fs. It follows that the biological water in the outer hydration shell was less labile than bulk water as its motion could be seen with our instruments. Around the hydrophilic AW residue at position 34, there are four charged or hydrophilic residues at positions 30, 31, 35, and 38 among the five proximate residues.[7] Therefore, the water molecules in the inner layer may form strong H-bonds with the charged (and hydrophilic) surface of the protein, affecting the H-bond networks in the outer hydration layers. Second, when normalized, the hydration dynamics of A1m-AW appeared to be slower than those of A1m in the initial 10 ps after photoexcitation. This may indicate that the extra H-bonding site of AW compared to that of W tended to retard water motion in the inner and outer hydration shells.

Third, the slowest hydration timescales were quite different: 50 ps for A1m and 380 ps for A1m-AW. This is thought to be due to the local protein (in)flexibility caused by the coupled water-proteins motion.[4b,c,f, 11] This is consistent with our observation that A1m-AW, which has a more hydrophilic residue (AW) than W that is directed opposite to the hydrophobic core of the coiled-coil structure, contains more α-helicity than A1m with a higher local

10.1002/ange.202002025

structural rigidity; it cannot be ruled out that the 380-ps component partly originated from the minor buried conformation of AW.

Discussion

The hydration results show that molecular interaction at hydrophilic surfaces reduces the mobility of water molecules, which increases the time required to break (and even longer to form) H-bonds. Note that bond breaking is unimolecular whereas bond formation is bimolecular and involves the formation of reactive encounter complexes. This effect appears to extend up to several hydration layers, which makes sense in that when the timescale of observation approaches that of the intrinsic dynamics, *i.e.*, the librational motion and the rotation of water molecules, the time constants no longer reflect thermodynamic aspects but instead represent those of molecular motion.

Our results demonstrate that it is possible to evaluate the free energy of H-bonds among biological water molecules at protein surfaces via the chemical kinetics approach. Here, the H-bond free energy of biological water was found to be 0.4 kcal/mol higher than that of bulk water. This is because highly structured H-bond networks in the vicinity of hydrophilic and charged protein surfaces may result in an entropic cost that dominates the free-energy difference. To validate the experimental approach, we applied Spoel's method[16] to calculate the difference in the free energy of H-bonds of biological water from that of bulk water using MD simulations. The kinetics of H-bond breakage and re-formation were investigated as per the following chemical-dynamics analysis. When the forward rate constant k for H-bond breakage and the backward rate constant k' for H-bond formation are defined, the kinetics of H-bonding can be described via the reactive flux correlation function $K(t)$:

$$K(t) = -\mathrm{d}c_h(t)/\mathrm{d}t = kc_h(t) - k'n(t), \quad (6)$$

where $c_h(t)$ is the autocorrelation function of the binary function $h(t)$, which is unity when a H-bond is present and zero otherwise. Note that H-bonds are counted when a donor and an acceptor are separated by a distance of 3.5 Å or less and the donor-H-acceptor angle is less than 30°. The term $n(t)$ represents the probability that a donor and an acceptor that have an H-bond at time zero will have a higher donor-H-acceptor angle than 30° but are still within the H-bonding distance. Based on the MD trajectories, the forward and backward rate constants were computed. The H-bond lifetime τ was calculated using the inverse of the forward rate constant. If we assume that the process of H-bond breakage can be described as an Eyring process, τ can be estimated from the Gibbs energy of activation $\Delta G^{\ddagger}$, where h is Planck's constant:

$$\tau = h/k_B T \exp(\Delta G^{\ddagger}/k_B T). \quad (7)$$

To compare the H-bond free energy between biological water and bulk water, τ and $\Delta G^{\ddagger}$ were calculated for each hydration shell around 7AI of AW and A1m-AW, the results of which are summarized in Table 1.

In the case of AW, the free energy required to break the H-bonds among water molecules was almost identical, *c.a.*, 1.6 kcal/mol, regardless of the distance between the water molecules and a residue surface. This confirms that AW is a suitable probe for measuring the free energy required to break H-bonds among water molecules in bulk. In the case of A1m-AW, the free energy to break H-bonds is similar to that of AW at the first hydration shell (r_{cut} = 4 Å). However, this energy gradually decreases as the radius of the hydration shell increases, which indicates that the free energy to break H-bonds among biological water molecules is smaller than that of bulk water molecules. It follows that the H-bond free energy of biological water molecules is higher than that of bulk water molecules as depicted in Figure 6. As the sensing distance of the probe residue is known to be up to 2 nm, we computed the difference of the H-bonding free energy ($\Delta\Delta G = \Delta G_{bio}^{\ddagger} - \Delta G_{bulk}^{\ddagger}$) by differentiating the respective radii of the hydration shell as 9, 14, and 20 Å, respectively. The calculated $\Delta\Delta G$ values at each hydration shell were −0.18, −0.29, and −0.33 kcal/mol, which are comparable to the measured $\Delta\Delta G$ value of −0.36 kcal/mol.

Table 1. Calculated H-bond lifetime (τ) and the activation energy to break H-bond between water molecules at each hydration layer of AW ($\Delta G_{bulk}^{\ddagger}$) and A1m-AW in the vicinity of probe residues ($\Delta G_{bio}^{\ddagger}$).

	AW		A1m-AW	
r_{cut} [Å]	τ [ps]	$\Delta G_{bulk}^{\ddagger}$ [kcal/mol]	τ [ps]	$\Delta G_{bio}^{\ddagger}$ [kcal/mol]
0~4	2.36 ± 0.08	1.60 ± 0.02	2.45 ± 0.22	1.62 ± 0.05
4~9	2.33 ± 0.02	1.59 ± 0.00	1.79 ± 0.12	1.43 ± 0.04
9~14	2.43 ± 0.05	1.61 ± 0.01	1.48 ± 0.05	1.32 ± 0.02
14~20	2.37 ± 0.01	1.60 ± 0.00	1.46 ± 0.02	1.31 ± 0.01
0~9	2.37 ± 0.01	1.60 ± 0.00	1.76 ± 0.15	1.42 ± 0.05
0~14	2.41 ± 0.00	1.61 ± 0.00	1.49 ± 0.04	1.32 ± 0.01
0~20	2.45 ± 0.00	1.62 ± 0.00	1.40 ± 0.01	1.29 ± 0.00

[a]Uncertainties were obtained from 5 independent MD trajectories as described in Supporting Information.

The results of the experiment and simulation show that in the hydrophilic and charged vicinity of AW in the A1m-AW protein, biological water has higher H-bond free energy than that of bulk water. This is in accordance with the results of previous research on the structure of water near a flat hydrophilic surface. Sandra and Dennis showed that with certain distances from hydrophilic surfaces, the hydration layer exhibits poor H-bonds compared with that of bulk water.[20] On the other hand, tetrahedrally ordered water has been reported near the charged residues at a protein surface.[21] In addition, the size of ions[22] and the topology of a local biological surface[23] have been reported to affect the H-bond network of water molecules in a diverse and complex way. For example, a small halide ion rarely perturbs the water network as much as a large halide ion. Likewise, a lower degree of surface curvature for a protein has been reported to affect the structure of hydration more than a high-curvature surface.

Even though extensive experiments and simulations have been performed over the past few decades to better understand the properties of water in biological environments,[4] information

10.1002/ange.202002025

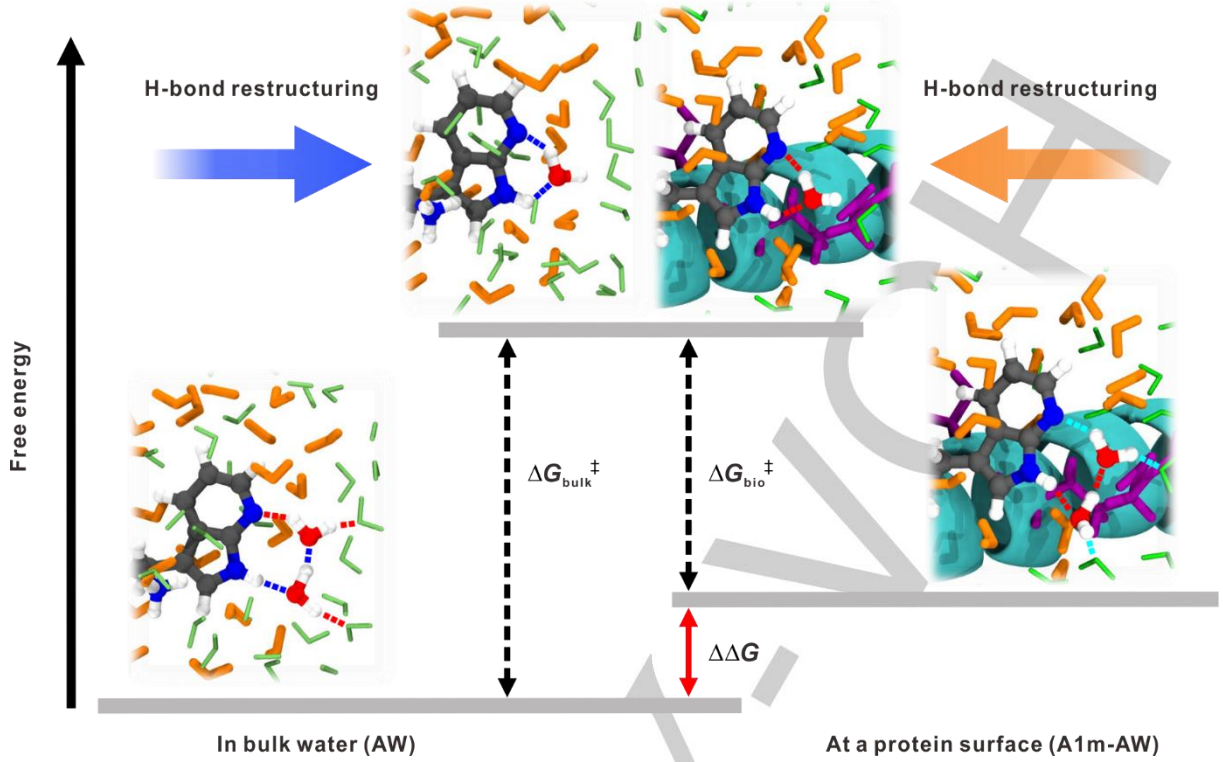

Figure 6. Schematic comparison of the H-bonding energetics of water in bulk and in the vicinity of the model protein surface probed by proton-transfer reaction to measure the H-bond free energy difference ($\Delta\Delta G$) between bulk water and biological water. Carbon, nitrogen, oxygen, and hydrogen atoms are displayed in gray, blue, red, and white, respectively. The water molecules in H-bond networks are depicted as orange-colored rods if they are in the inner hydration layer of AW and as green-colored rods otherwise. The hydrophilic residues at A1m-AW protein are displayed as purple rods.

on the H-bond energy of local biological water is scarce and what exists is mostly based on simulations utilizing computational methodologies reporting its diverse characteristics determined by many factors.[24] To address the lack of information, we leveraged the selective localization of the unique probe at protein surfaces of interest to glimpse the energetic (and dynamic) properties of local biological water. We anticipate our proposed approach to be applicable to locally map diverse roles of such water in structural integrity, assembly, change, and function of proteins.

Conclusions

In this paper, we introduced a new experimental approach to evaluate the H-bond free energy of water at protein surfaces. By tracking the well-established photoinduced prototropy of the fluorescent residue of 7-azatryptophan, which is the non-canonical isostere of tryptophan, at protein surfaces and in bulk water, the ratio of the water-catalyzed proton-transfer rates was rationalized as a measure for estimating the difference in the free energy associated with the H-bond network around the fluorescent hydration probe. In this way, we determined that the H-bond free energy of biological water in this study was higher than that of bulk water by 0.4 kcal/mol. The difference may be due to the entropic cost of the highly structured H-bond network in the vicinity of the hydrophilic and charged protein surfaces. In the future, we plan to install fluorescent probes at desired locations in proteins via molecular biology and protein engineering techniques to elucidate the detailed H-bond energetics/dynamics properties of local biological water on various topological and hydrophobic-against-hydrophilic surfaces.

Acknowledgements

This work was supported by the National Research Foundation of Korea (NRF) funded by the Ministry of Science, ICT and Future Planning (2014R1A1A1008289 and 2014R1A5A1009799), Ministry of Education (2019R1A6A1A11051471), and by the Institute for Basic Science (IBS-R020-D1), Korea. The computational resources were provided by UNIST-HPC and KISTI (KSC-2016-C2-0062).

Keywords: Biological water • Femtochemistry • Hydrogen-bond free energy • Protein engineering • Proton transfer

[1] a) P. Ball, *Chem. Rev.* **2008**, *108*, 74-108; b) Y. Levy, J. N. Onuchic, *Annu. Rev. Biophys. Biomol. Struct.* **2006**, *35*, 389-415; c) H. Frauenfelder, G. Chen, J. Berendzen, P. W. Fenimore, H. Jansson, B. H. McMahon, I. R. Stroe, J. Swenson, R. D. Young, *Proc. Natl. Acad. Sci. U. S. A.* **2009**, *106*, 5129-5134; d) S. K. Pal, A. H. Zewail, *Chem. Rev.* **2004**, *104*, 2099-2124; e) L. Wang, X. Yu, P. Hu, S. Broyde, Y. Zhang, *J.*

10.1002/ange.202002025

Am. Chem. Soc. **2007**, *129*, 4731-4737; f) B. Jayaram, T. Jain, *Annu. Rev. Biophys. Biomol. Struct.* **2004**, *33*, 343-361; g) M.-C. Bellissent-Funel, A. Hassanali, M. Havenith, R. Henchman, P. Pohl, F. Sterpone, D. van der Spoel, Y. Xu, A. E. Garcia, *Chem. Rev.* **2016**, *116*, 7673-7697.

[2] a) P. Ball, *Proc. Natl. Acad. Sci. U. S. A.* **2017**, *114*, 13327-13335; b) J. Schiebel, R. Gaspari, T. Wulsdorf, K. Ngo, C. Sohn, T. E. Schrader, A. Cavalli, A. Ostermann, A. Heine, G. Klebe, *Nat. Commun.* **2018**, *9*, 3559; c) J. F. Darby, A. P. Hopkins, S. Shimizu, S. M. Roberts, J. A. Brannigan, J. P. Turkenburg, G. H. Thomas, R. E. Hubbard, M. Fischer, *J. Am. Chem. Soc*. **2019**, *141*, 15818-15826.

[3] a) D. Zhong, S. K. Pal, A. H. Zewail, *Chem. Phys. Lett.* **2011**, *503*, 1-11; b) K. Bhattacharyya, *Chem. Commun.* **2008**, 2848-2857; c) S. Mahatabuddin, D. Fukami, T. Arai, Y. Nishimiya, R. Shimizu, C. Shibazaki, H. Kondo, M. Adachi, S. Tsuda, *Proc. Natl. Acad. Sci. U. S. A.* **2018**, *115*, 5456-5461.

[4] a) W.-C. Chao, J.-Y. Shen, J.-F. Lu, J.-S. Wang, H.-C. Yang, K. Wee, L.-J. Lin, Y.-C. Kuo, C.-H. Yang, S.-H. Weng, H.-C. Huang, Y.-H. Chen, P.-T. Chou, *J. Phys. Chem. B* **2015**, *119*, 2157-2167; b) Y. Qin, L. Wang, D. Zhong, *Proc. Natl. Acad. Sci. U. S. A.* **2016**, *113*, 8424-8429; c) O.-H. Kwon, T. H. Yoo, C. M. Othon, J. A. Van Deventer, D. A. Tirrell, A. H. Zewail, *Proc. Natl. Acad. Sci. U. S. A.* **2010**, *107*, 17101-17106; d) N. Nandi, B. Bagchi, *J. Phys. Chem. B* **1997**, *101*, 10954-10961; e) A. Chowdhury, S. A. Kovalenko, I. V. Aramburu, P. S. Tan, N. P. Ernsting, E. A. Lemke, *Angew. Chem. Int. Ed.* **2019**, *58*, 4720-4724; f) J. Yang, Y. Wang, L. Wang, D. Zhong, *J. Am. Chem. Soc*. **2017**, *139*, 4399-4408.

[5] a) Y. Chen, R. L. Rich, F. Gai, J. W. Petrich, *J. Phys. Chem*. **1993**, *97*, 1770-1780; b) P. Ilich, *J. Mol. Struct.* **1995**, *354*, 37-47; c) O.-H. Kwon, A. H. Zewail, *Proc. Natl. Acad. Sci. U. S. A.* **2007**, *104*, 8703-8708; d) O.-H. Kwon, Y.-S. Lee, H. J. Park, Y. Kim, D.-J. Jang, *Angew. Chem. Int. Ed.* **2004**, *43*, 5792-5796; e) S. Takeuchi, T. Tahara, *Proc. Natl. Acad. Sci. U. S. A.* **2007**, *104*, 5285-5290; f) Y.-S. Wu, H.-C. Huang, J.-Y. Shen, H.-W. Tseng, J.-W. Ho, Y.-H. Chen, P.-T. Chou, *J. Phys. Chem. B* **2015**, *119*, 2302-2309; g) P.-T. Chou, W.-S. Yu, C.-Y. Wei, Y.-M. Cheng, C.-Y. Yang, *J. Am. Chem. Soc*. **2001**, *123*, 3599-3600.

[6] a) S. Mente, M. Maroncelli, *J. Phys. Chem. A* **1998**, *102*, 3860-3876; b) O.-H. Kwon, D.-J. Jang, *J. Phys. Chem. B* **2005**, *109*, 20479-20484.

[7] a) J. K. Montclare, S. Son, G. A. Clark, K. Kumar, D. A. Tirrell, *ChemBioChem* **2009**, *10*, 84-86; b) W. A. Petka, J. L. Harden, K. P. McGrath, D. Wirtz, D. A. Tirrell, *Science* **1998**, *281*, 389-392.

[8] C. Louis-Jeune, M. A. Andrade-Navarro, C. Perez-Iratxeta, *Proteins: Struct., Funct., Bioinf.* **2012**, *80*, 374-381.

[9] a) J. T. Vivian, P. R. Callis, *Biophys. J.* **2001**, *80*, 2093-2109; b) Y.-T. Chen, W.-C. Chao, H.-T. Kuo, J.-Y. Shen, I. H. Chen, H.-C. Yang, J.-S. Wang, J.-F. Lu, R. P. Cheng, P.-T. Chou, *Biochem. Biophys. Rep.* **2016**, *7*, 113-118.

[10] J. Guharay, P. K. Sengupta, *Biochem. Biophys. Res. Commun.* **1996**, *219*, 388-392.

[11] W. Qiu, L. Zhang, O. Okobiah, Y. Yang, L. Wang, D. Zhong, A. H. Zewail, *J. Phys. Chem. B* **2006**, *110*, 10540-10549.

[12] B. Valeur, M. N. Berberan-Santos, in *Molecular Fluorescence*, Wiley-VCH Verlag GmbH & Co. KGaA, **2012**, pp. 181-212.

[13] R. L. Rich, A. V. Smirnov, A. W. Schwabacher, J. W. Petrich, *J. Am. Chem. Soc.* **1995**, *117*, 11850-11853.

[14] C. F. Chapman, M. Maroncelli, *J. Phys. Chem.* **1992**, *96*, 8430-8441.

[15] S. J. Strickler, R. A. Berg, *J. Chem. Phys.* **1962**, *37*, 814–822.

[16] D. van der Spoel, P. J. van Maaren, P. Larsson, N. Tîmneanu, *J. Phys. Chem. B* **2006**, *110*, 4393-4398.

[17] Y. Marcus, *Chem. Rev.* **2009**, *109*, 1346-1370.

[18] W. Lu, J. Kim, W. Qiu, D. Zhong, *Chem. Phys. Lett.* **2004**, *388*, 120-126.

[19] a) V. Conti Nibali, M. Havenith, *J. Am. Chem. Soc.* **2014**, *136*, 12800-12807; b) T. Li, A. A. Hassanali, Y.-T. Kao, D. Zhong, S. J. Singer, *J. Am. Chem. Soc.* **2007**, *129*, 3376-3382.

[20] S. Roy, D. K. Hore, *J. Phys. Chem.* C **2012**, *116*, 22867-22877.

[21] P. Rani, P. Biswas, *J. Phys. Chem. B* **2015**, *119*, 10858-10867.

[22] M. F. Kropman, H. J. Bakker, *Science* **2001**, *291*, 2118.

[23] J. T. King, E. J. Arthur, C. L. Brooks, K. J. Kubarych, *J. Phys. Chem. B* **2012**, *116*, 5604-5611.

[24] a) H. Yu, S. W. Rick, *J. Am. Chem. Soc.* **2009**, *131*, 6608-6613; b) B. Breiten, M. R. Lockett, W. Sherman, S. Fujita, M. Al-Sayah, H. Lange, C. M. Bowers, A. Heroux, G. Krilov, G. M. Whitesides, *J. Am. Chem. Soc.* **2013**, *135*, 15579-15584.

10.1002/ange.202002025

WILEY-VCH

RESEARCH ARTICLE

Entry for the Table of Contents

RESEARCH ARTICLE

A new experimental approach for estimating H-bond free energy of local biological water has been proposed. This was made possible by combining time-resolved spectroscopy and protein engineering, with installing a fluorescent, prototropic hydration probe at protein surfaces. This study promises the access to energetics and dynamics of local biological water at protein surfaces of interest.

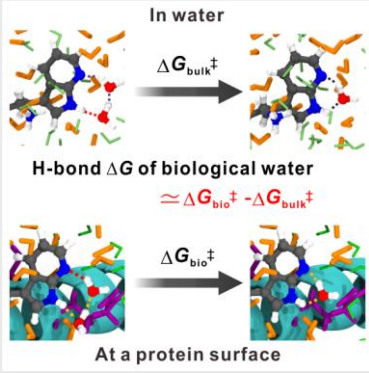

Won-Woo Park[a], *Kyung Min Lee*[b], *Byeong Sung Lee*[c], *Young Jae Kim*[a,d], *Se Hun Joo*[b], *Sang Kyu Kwak*[*,b], *Tae Hyeon Yoo*[*,c], *and Oh-Hoon Kwon*[*,a,d]

Page No. – Page No.

Title : Hydrogen-Bond Free Energy of Local Biological Water